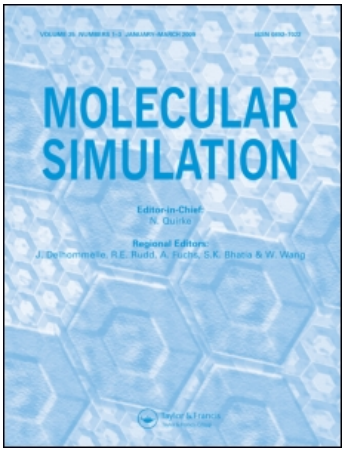

Molecular Simulation
Publication details, including instructions for authors and subscription information:
http://www.informaworld.com/smpp/title~content=t713644482

Molecular Dynamics Simulation of Self Diffusion in Microclusters

Masahumi Okada[a]; Hiromitsu Yoshimoto[b]; Kazumi Nishioka[b]
[a] Industrial Technology Center of Tokushima, Tokushima, Japan [b] Faculty of Engineering, University of Tokushima, Tokushima, Japan

To cite this Article Okada, Masahumi , Yoshimoto, Hiromitsu and Nishioka, Kazumi(1995) 'Molecular Dynamics Simulation of Self Diffusion in Microclusters', Molecular Simulation, 14: 2, 67 — 81
To link to this Article: DOI: 10.1080/08927029508022008
URL: http://dx.doi.org/10.1080/08927029508022008

Molecular Simulation, 1995, Vol. 14, pp. 67–81
Reprints available directly from the publisher
Photocopying permitted by license only

MOLECULAR DYNAMICS SIMULATION OF SELF DIFFUSION IN MICROCLUSTERS

MASAHUMI OKADA, HIROMITSU YOSHIMOTO* and KAZUMI NISHIOKA*

Industrial Technology Center of Tokushima, 11-2 Saiga, Tokushima 770, Japan
**Faculty of Engineering, University of Tokushima, 2-1 Minamijosanjima Tokushima 770, Japan*

(Received July 1994, accepted July 1994)

Molecular dynamics simulation is carried out to study the mechanism of self diffusion which is characteristic of solid-like microclusters. A two-dimensional system with the Lennard-Jones potential is employed and the temperatures near the triple point of the two-dimensional bulk system are adopted for the simulation. The results show that: a) microclusters consist of two regions, i.e., solid-like cores and liquid-like surface regions, b) the size dependence of the diffusion coefficient for microclusters is weak, and the value of the solid-like core region is not much different from that of the bulk liquid, c) the activation energy of diffusion for microclusters is twenty to thirty times larger than that for the bulk liquid, d) the diffusion mechanism in the solid-like region involves the collective motion of small domains containing ten to twenty atoms which results in the formation of low density regions, sometimes even vacancy clusters, between them, and atoms in the low density regions change their positions to cause diffusion.

KEY WORDS: Microcluster, diffusion, molecular dynamics simulation.

1 INTRODUCTION

It was found experimentally by Kaito and coworkers [1,2] that ordered crystalline phases of Fe and Ni including tetrataenite can be produced by coalescence growth [3,4,5,6] of ultrafine crystallites of Fe and Ni with 10–40 nm in diameter which are produced by the gas evaporation technique [7]. The coalescence takes place in a short time ($10^{-2} - 10^{-3}$ s) when crystallites of Fe and Ni in the atmosphere of an inert gas are heated to temperature above 473 K. The ordered phases of Fe–Ni system can be produced also by the reaction between a thin film and a crystallite when the system is annealed at 537 K for 1 hour [8]. Tetrataenite has the ordered tetragonal structure with 50%Fe-50%Ni in atomic ratio and it has been found in meteorites. However, it had not been possible to produce it experimentally before the works by Katio and coworkers except by neutron irradiation in the presence of a magnetic field [9] or by electron beam irradiation [10] of the ordinary disordered taenite crystal.

Formation of ordered crystalline alloy phases by coalescence of ultrafine crystallites of Fe and Ni implies that diffusion takes place during the process. However, if we employ diffusion coefficient of Ni atoms in bulk Fe crystal or of Fe atoms in bulk Ni crystal to estimate the time required for the process, it will be on the order of 10^6 years or more. This means that intermixing of atoms in ultrafine crystallites occurs many orderes of magnitude faster than in the bulk crystals. There may be a possibility that

melting or quasimolten state [11] is achieved for crystallites due to the size effect. However, considering the size range of 10–40 nm, which is rather large for the size effect on melting to be important, and the temperature as low as 473 K, it is likely that crystallites remain to be in crystalline phase [12]. This suggests that diffusion mechanism being characteristic of ultrafine crystallites operates to cause high diffusivity.

Recently Mori *et al.* [13] found, by transmission electron microscopic studies, another interesting phenomenon that homogeneous alloying of copper with gold takes place in less than 30 s, which corresponds to the time required to do the experiment, at room temperature in gold clusters of about 10 nm in diameter. In those experiments, the isolated gold clusters were first prepared on a supporting amorphous carbon film by vapor deposition, then copper atoms were deposited onto the film (and of course onto the gold clusters) which was kept at room temperature. Diffusion coefficient of Cu in Au clusters estimated to explain this phenomenon is at least nine orders of magnitude larger than that of the bulk value [13]. This result was confirmed by the in situ experiment of Yasuda *et al.* [14]. Similarly, homogeneous alloying of Au in Cu clusters of about 4 nm was also found at room temperature [15], and the diffusion coefficient of Au in Cu clusters is estimated to be 19 orders of magnitude larger than that of the bulk value in this case.

Yasuda *et al.* [16] extended the experiments of alloying Au clusters with Cu atoms by reducing the temperature to 245, 215, 165 and 125 K. In those experiments, isolated gold clusters of about 4 nm in diameter were prepared on a supporting film at room temperature, then the film was cooled to the above mentioned temperatures during the Cu deposition. At 245 K homogeneous alloying of clusters was observed as was done at room temperature, but the results at 215 and 165 K were interpreted as the following: 1) the dissolution of Cu takes place only in the shell-shaped region beneath the surface of individual gold clusters and the central part is left as pure gold, 2) thickness of the shell-shaped region decreases with decreasing temperature. At 125 K clusters remained pure gold even after the deposition of Cu onto them, and this was interpreted that the thickness of the shell-shaped region becomes practically zero at this temperature. The state of clusters remained unchanged even after aging the specimens up to 28.8 ks at the temperatures at which Cu depositions were done. To explain those results, diffusion coefficients in clusters must be many orders of magnitude larger than that of the bulk crystal.

Those experiments were further extended to systems in which intermetallic compound may be formed. Yasuda and Mori [17] found that deposition of Zn onto nm-sized gold clusters at room temperature quickly changed them into Au–Zn solid solution, disordered $\alpha_1 - Au_3Zn$ or ordered $\beta' - AuZn$ clusters depending on the amount of deposited zinc. The zinc diffusivity in gold clusters estimated for the results is at least 10 orders of magnitude larger than that of the bulk. Mori and Yasuda [18] studied alloying behavior of antimony atoms into nm-sized gold clusters and that of gold atoms into nm-sized antimony clusters. During the experiments, clusters were supported on a carbon film that was kept at room temperature. In both cases, vapor-deposited solute atoms quickly dissolved into the clusters to form the intermetallic compound $AuSb_2$ whose melting temperature in bulk is 733 K. The estimated diffusivity of Sb in nm-sized Au clusters is again at least 10 orders of magnitude larger than that of the bulk.

Thus, both of the two series of experiments described above suggest that the diffusivity in clusters must be many orders of magnitude larger than that in the bulk crystal. To understand the reason behind it and to get the insight into the diffusion mechanisms which are characteristic to microclusters, we expect that the molecular dynamics simulation may provide essential information, and the present work aims at doing it. We employ two-dimensional system of atoms interacting with the Lennard-Jones potential in the present paper rather than three dimensional systems with potentials which are more realistic for the experimentally investigated systems. We regard the observation of the animated motion of atoms as crucially important in gaining insight to the problem, and the employment of two-dimensional systems is essential to achieve this purpose. Since qualitative understanding toward the nature of the problem is aimed as the first step, the Lennard-Jones potential is considered to be sufficient. Further, we study self-diffusion in single component clusters instead of interdiffusion in binary systems in the present paper.

2 PROCEDURE OF SIMULATION

We use the molecular dynamics method of simulation and to represent the atomic interaction we employ the Lennard-Jones potential

$$\phi(r_{ij}) = 4\varepsilon\left\{\left(\frac{\sigma}{r_{ij}}\right)^{12} - \left(\frac{\sigma}{r_{ij}}\right)^{6}\right\}, \tag{1}$$

where ε denotes the depth, σ the interatomic separation where the potential takes the value zero and r_{ij} the distance between the atoms i and j. We employed the Verlet algorithm for integration with a time step of $\tau/25$, where τ represents

$$\tau = \sqrt{\frac{m\sigma^2}{4\varepsilon}}, \tag{2}$$

in which m denotes the mass of an atom. The Cut-off radius R_c is 3.5σ.

We prepare the model for a cluster by arranging atoms in a hexagonal shape with the lattice constant of the bulk crystal at 0 K and assigning them velocities under the condition that the total linear and angular momenta vanish. We represent the nominal size of a cluster as $C(N_c)$, where N_c denotes the number of atoms on an edge of a hexagon. The total number N contained in a cluster is related to N_c as $N = 3N_c(N_c - 1) + 1$. The actual size for which the data are taken may be slightly smaller than the nominal size due to evaporation of atoms. We place the cluster in a square with the preiodic boundary and raise the temperature to the desired value by proportionally increasing the velocities of atoms. The temperatures adopted are 0.417, 0.375 and 0.333 in the unit of ε/k_B, where k_B denotes Boltzmann's constant. After the temperature reached the desired value, it is adjusted at every time step for the first 1000 steps for aging, then the system is isolated afterwards. Typically about ten to twenty atoms evaporate and recondense in 3000 steps at $T = 0.417\varepsilon/k_B$, several atoms at $T = 0.375\varepsilon/k_B$ and negligible at $0.333\varepsilon/k_B$. We exclude those atoms in analyzing the data. Changes in the linear and angular momenta of a cluster due to evaporation and

recondensation at the temperatures adopted are negligible as seen in the well-defined lattice points in the trajectories in Figure 1. However, fragmentation of smaller clusters inhibits the study on the size dependence of the diffusion coefficient at higher temperatures. As seen in Figure 2 the systems are in equilibrium after the aging process and the fluctuation from one "phase" to the other "phase" as found by Jellinek *et al.* [11] was not observed in 1555τ steps in the present simulation.

For comparison, simulation of the bulk liquid is done with a system which consists of 200 atoms under the preiodic boundary condition at $T = 0.417\varepsilon/k_B$. The size of the system is chosen so that the pressure is about $0.007\varepsilon/\sigma^2$, which is near the pressure at the triple point. At $T = 0.375$ or $0.333\varepsilon/k_B$ bulk liquid state could not be obtained in the present simulation. These temperatures are lower than that of the triple point [19] for the two-dimensional Lennard-Jones system.

3 RESULTS AND DISCUSSION

3.1 Diffusion coefficient

The mean square displacements of atoms vs time for a cluster with the size $C(11)$ at $T = 0.375\varepsilon/k_B$ are shown in Figures 3a and 3b as typical examples. Note that the results are roughly linear. Figure 3a shows the mean square displacement for the whole cluster and Figure 3b for the atoms initially inside a classifying circle given in Figure 4. The classifying circle is chosen so that at $T = 0.417\varepsilon/k_B$ the trajectories outside it indicate

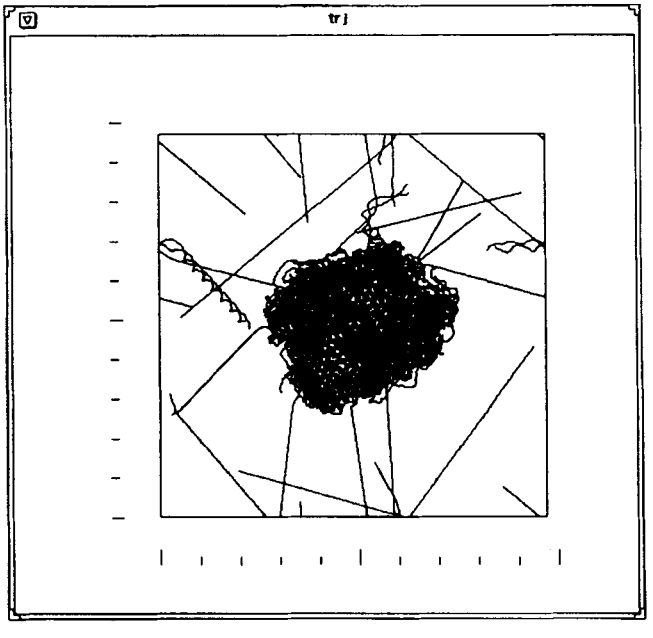

Figure 1a A trajectory plot over $77\,\tau$ at $T = 0.417\varepsilon/k_B$.

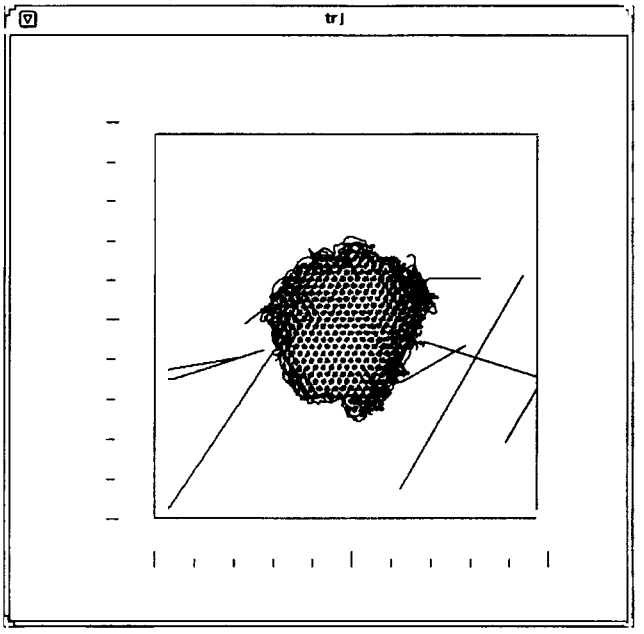

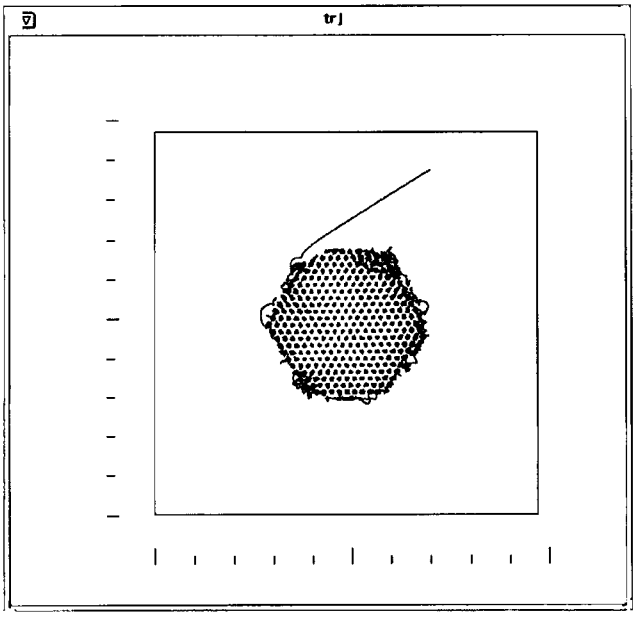

Figure 1c A trajectory plot over 77 τ at $T = 0.333\varepsilon/k_B$.

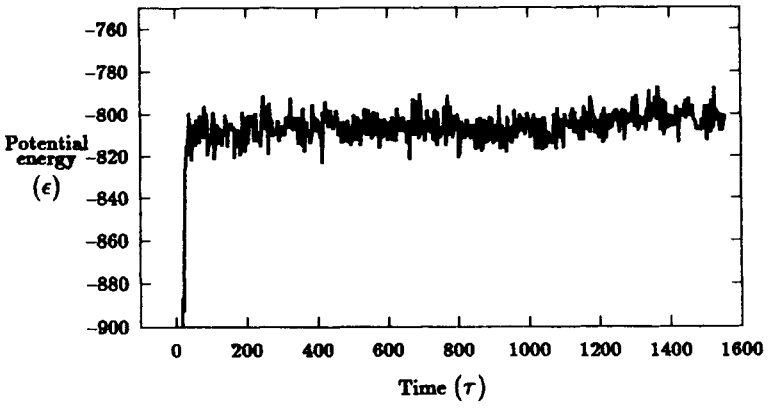

Figure 2 Change of the potential energy over 1555τ at $T = 0.375\varepsilon/k_B$.

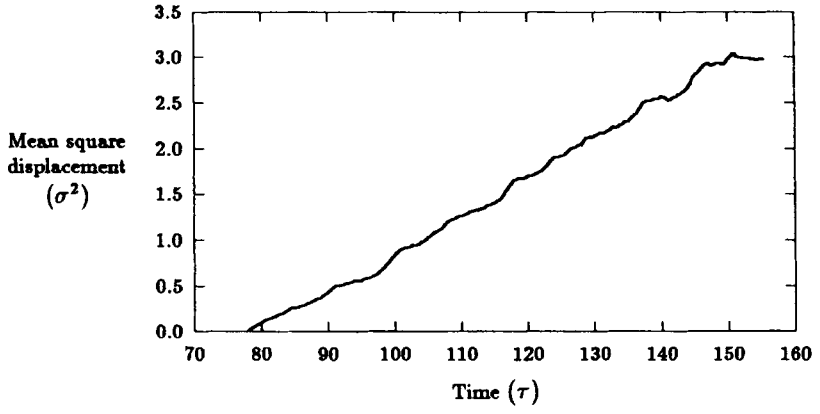

Figure 3a The mean square displacement vs time for the whole cluster at $T = 0.375\varepsilon/k_B$.

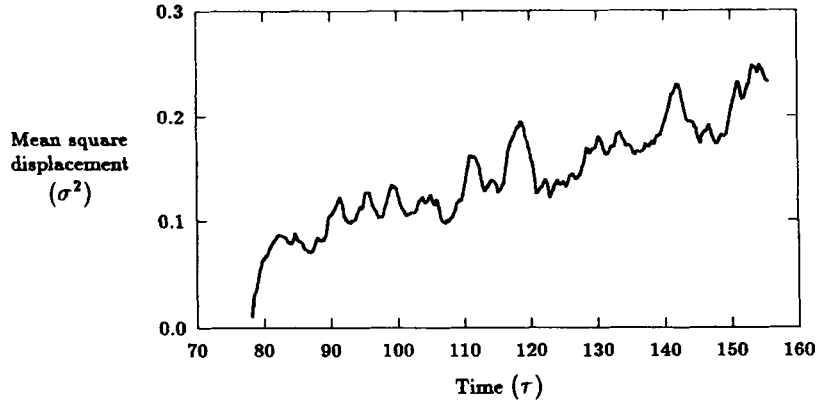

Figure 3b The mean square displacement vs time for the atoms inside the classifying circle at $T = 0.375\varepsilon/k_B$.

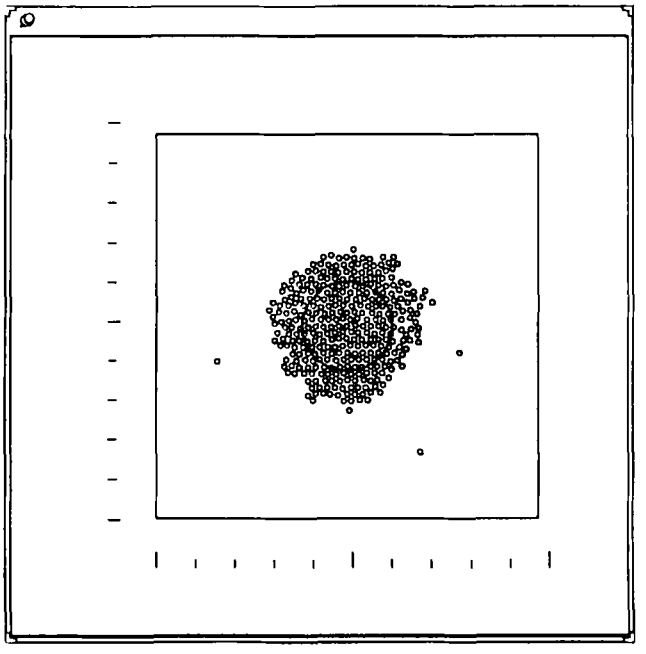

Figure 4 A snapshot of a cluster in equilibrium at $T = 0.375\varepsilon/k_B$ and the classifying circle.

strong liquid-like behavior. For each cluster size the same classifying circle is used also for lower temperatures. Self diffusion coefficient D is related to the mean square displacements by

$$D = \lim_{t \to \infty} \frac{1}{4t} \langle |\vec{r}(t) - \vec{r}(0)|^2 \rangle, \tag{3}$$

where $\vec{r}(0)$ and $\vec{r}(t)$ represent position vectors of an atom at the initial time and at time t, respectively, and $\langle\ \rangle$ means the average over the atoms. The values of D are obtained from the slopes of the graphs such as those in Figures 3a and 3b by the least squares fitting. The results are shown in Figures 5 and 6 at the temperatures 0.417 and $0.375\varepsilon/k_B$, respectively.

Three data were taken for each nominal size by assigning distinct sets of the initial velocities which were sampled from the same Maxwell-Boltzmann distribution. Open circles indicate the results for whole clusters and dots for the regions inside the classifying circles. For smaller clusters, $C(5)$, $C(6)$ and $C(7)$, only the open circles are shown, because it was difficult to define the classifying circles in those cases. At $T = 0.333\varepsilon/k_B$, the diffusion coefficient was found to be negligibly small. We see in Figures 5 and 6 that the results for clusters scatter especially for the smaller size range whereas the scatter for the bulk is negligible as shown in Figure 5 in spite of the fact that in evaluating the diffusion coefficient the number of atoms and the time duration are about the same for both cases. This suggests that the scatter found for clusters results from the statistical fluctuation inherent in the diffusion mechanism for clusters. As

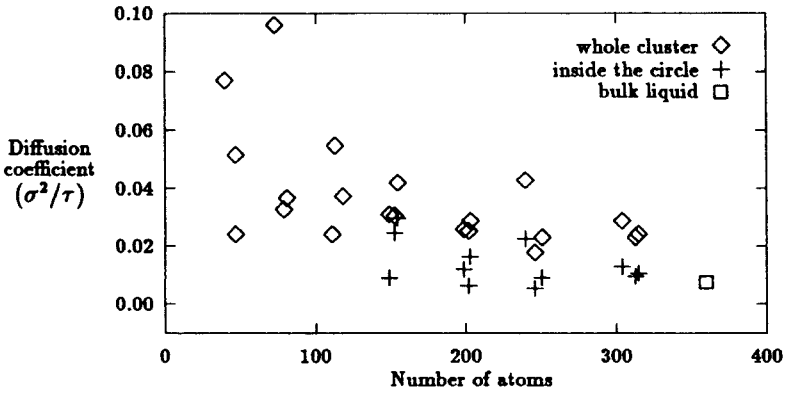

Figure 5 The diffusion coefficient vs cluster size at $T = 0.417\varepsilon/k_B$.

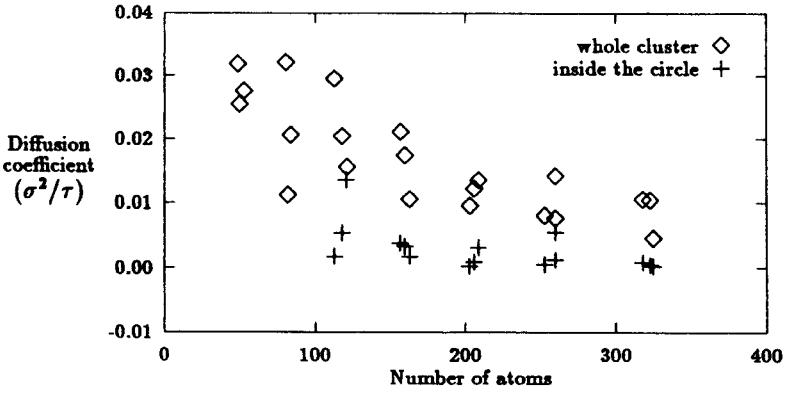

Figure 6 The diffusion coefficient vs cluster size at $T = 0.375\varepsilon/k_B$.

regards the data for larger clusters, the value of D in the region inside the classifying circle of each cluster has strong correlation with that for the whole cluster. This suggests that the diffusive motion inside the classifying circle is strongly influenced by the motion of atoms in the surface region.

We see in Figure 5 that the size dependence of the diffusion coefficient is very weak. Note that the diffusion coefficient for the bulk liquid, which is found to be $7.39 \times 10^{-3}\sigma^2/\tau$, is only slightly smaller than the average value of about $1.10 \times 10^{-2}\sigma^2/\tau$ for the clusters when the values for the region inside the classifying circles are adopted. The values for whole clusters are several times larger than those for the region inside the classifying circles. Note also in Figure 6, which shows the results at $T = 0.375\varepsilon/k_B$, that the values of D for the region inside the classifying circles are not much smaller, i.e., only about two orders of magnitude smaller, than that for the bulk liquid at $T = 0.417\varepsilon/k_B$. This is very important when we take into consider-

ation that the region inside the classifying circles is found to be solid-like as to be discussed later.

3.2 *Activation energy*

To get information on the possible difference of the diffusion mechanism between the bulk liquid and the clusters, we calculated the activation energies for each case. Supposing that the temperature dependence of the diffusion coefficient for clusters takes the following form of a thermally activated process,

$$\log_e(D) \propto \log_e(D_0) - \frac{E_a}{k_B T}, \tag{4}$$

we evaluate the activation energy E_a from the slope of $\log_e(D)$ vs $1/T$. The results are given in Figure 7. Temperatures adopted for the bulk liquid are $T = 0.417, 0.459$ and $0.500\varepsilon/k_B$ and the number density of atoms $0.751/\sigma^2$ is adopted for all cases. For clusters, $T = 0.417$, 0.375 and $0.333\varepsilon/k_B$ are employed, and the data for the whole clusters are adopted. We see a linear relation for the bulk liquid and an approximate linearity for the clusters. Each point for clusters represents the avarage of three data. We see that the slopes for clusters are much steeper than that for the bulk liquid.

3.3 *Velocity auto-correlation function and spectral analysis*

Normalized velocity auto-correlation function is given by

$$\psi(t) = \frac{\langle \vec{v}(t_0 + t) \cdot \vec{v}(t_0) \rangle}{\langle \vec{v}(t_0) \cdot \vec{v}(t_0) \rangle}, \tag{5}$$

where $\vec{v}(t)$ denotes the velocity of an atom at time t and the average is to be taken over atoms and also over the base time t_0. The results are shown in Figures 8, 9 and 10.

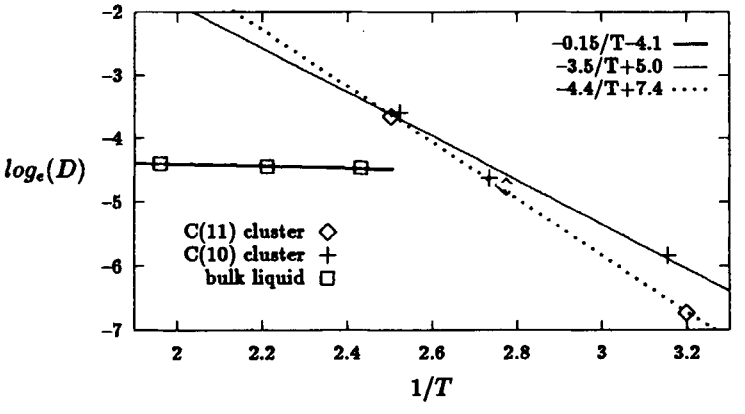

Figure 7 The diffusion coefficient vs $1/T$ for clusters and for the bulk liquid. D and T are in the units of σ^2/τ and ε/k_B, respectively.

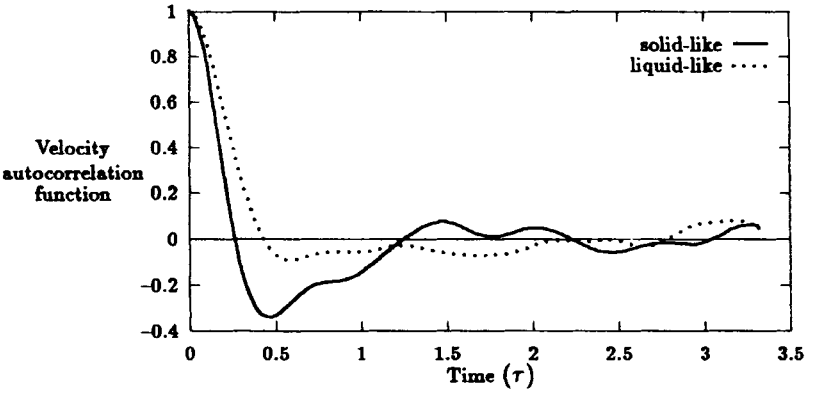

Figure 8 The normalized velocity autocorrelation functions in solid-like and liquid-like bulks at $T = 0.417\varepsilon/k_B$.

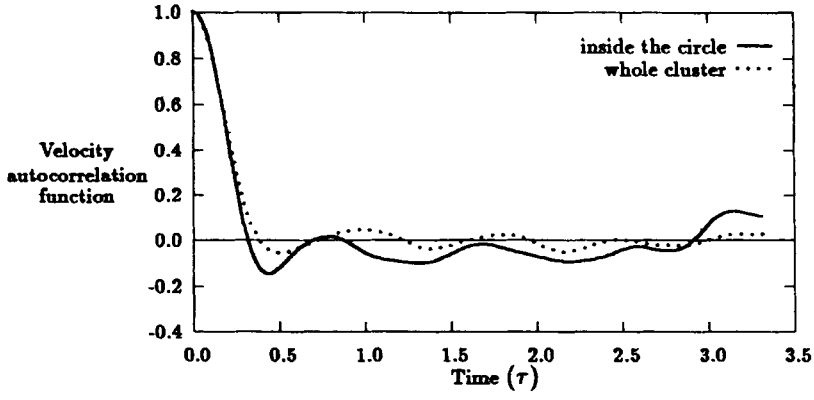

Figure 9 The normalized velocity autocorrelation functions in the whole cluster and inside the circle of a cluster $C(11)$ at $T = 0.417\varepsilon/k_B$.

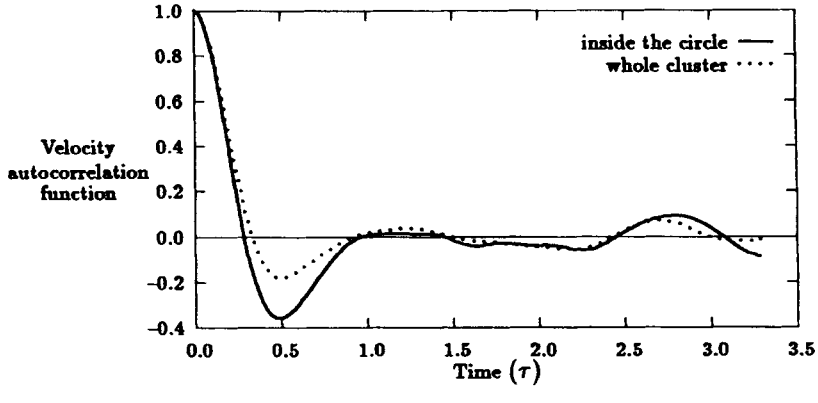

Figure 10 The normalized velocity autocorrelation functions in the whole cluster and inside the circle of a cluster $C(11)$ at $T = 0.375\varepsilon/k_B$.

Figure 8 shows the results for solid-like and liquid-like bulks at $T = 0.417\varepsilon/k_B$, in which a slightly larger density is adopted to get the bulk solid state. The two curves indicate typical features of the bulk solid and of the bulk liquid, respectively. Figures 9 and 10 show the results for the whole cluster and for the region inside the classifying circle of a cluster $C(11)$ at $T = 0.417\varepsilon/k_B$ and at $T = 0.375\varepsilon/k_B$, respectively. In those results the difference between the curves for the whole cluster and for the region inside the classifying circle is not clear.

Fourier transformation of Figures 8, 9 and 10 are shown in Figures 11, 12 and 13, respectively. We numerically integrated the following equation:

$$I(\omega) = 2\int_0^\infty \psi(t)\cos(\omega t)dt, \tag{6}$$

where ω denotes the angular frequency. As well known, density at zero frequency indicates diffusion. Figure 11 presumably shows typical spectra of bulk solid and of

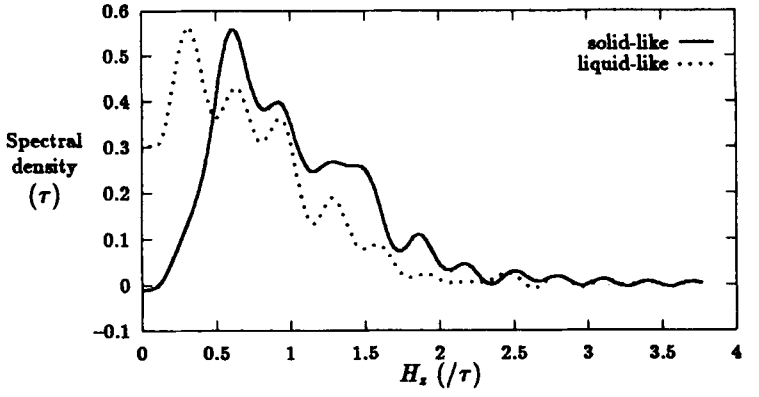

Figure 11 The power spectra obtained from the curves of Figure 8.

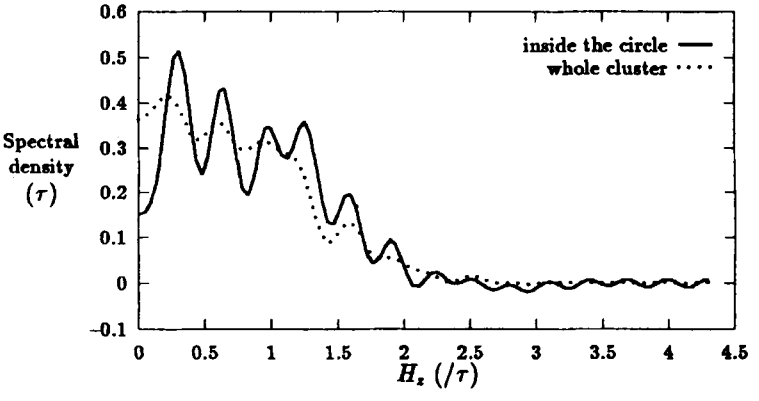

Figure 12 The power spectra obtained from the curves of Figure 9.

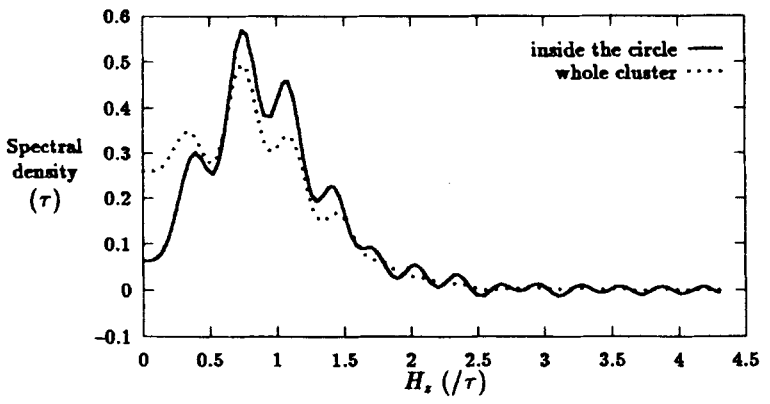

Figure 13 The power spectra obtained from the curves of Figure 10.

bulk liquid. Note that the solid curve does not have density at zero frequency whereas the dotted curve has appreciable density there. In Figure 12, the whole cluster shows liquid at $T = 0.417\varepsilon/k_B$, but inside the classifying circle we observe solid-like property. However, as seen in Figure 13, the two curves approach when the temperature is decreased.

3.4 *Visual analysis*

As stated in INTRODUCTION, we regard the visual analysis on the motion of atoms as crucially important in gaining insight into the mechanism of diffusion in microclusters. For this purpose we developed the visual-information software system which possesses the functions of showing distributions of the normalized correlated motion coefficient and the squared displacement of atoms as well as for animation, trajectory and snapshot. As seen in the trajectories shown in Figures 1b and 1c, surface melting is observed at these temperatures which are in the solid phase region for the bulk. This is consistent with the normalized velocity autocorrelation functions and the power spectra shown in Figures 10 and 13. At $T = 0.417\varepsilon/k_B$ which is in the liquid phase region for the bulk, Figure 1a shows that the solid-like domains coexist with the liquid-like domains as mentioned already.

Employing the function for animation, it is observed in clusters at $T = 0.375\varepsilon/k_B$ that collective motion of solid-like domains containing ten to twenty atoms occurs which results in the formation of low density regions, sometimes even vacancy clusters, between them. Atoms in the low density regions change their positions to cause diffusion. Life time of the individual domain and individual low density region is rather short, and other domains and other low density regions are subsequently introduced. Formation and collective motion of domains seems to have correlation with the vigorous thermal motion of liquid-like region at the surface.

As a method to represent collective motion of atoms, we employed the normalized correlated motion coefficient, which is a modification of the parameter introduced

recently by Muranaka and Hiwatari [20]. It is defined as:

$$c_i = \frac{1}{N_r} \sum_{\{j \mid |\vec{r}_i(t_0) - \vec{r}_j(t_0)| \leq R_c\}}^{N_r} \frac{\Delta \vec{r}_i}{|\Delta \vec{r}_i|} \cdot \frac{\Delta \vec{r}_j}{|\Delta \vec{r}_j|}, \tag{7}$$

where the subscripts i and j indicate i'th and j'th atoms, respectively, N_r denotes the number of atoms within the circle with the radius R_c which is chosen to be 2.50σ. $\Delta \vec{r}_i$ is defined as $\Delta \vec{r}_i = \vec{r}_i(t_0 + t) - \vec{r}_i(t_0)$ and t is chosen to be 60τ. Figure 14 shows the distribution of the normalized correlated motion coefficient in a cluster at $T = 0.375\varepsilon/k_B$. We see one large domain of atoms with the highest correlation. However, this is quite different from the impression of the observation of animation. As described already, smaller domains show respective collective motions which result in the formation of low density region between them. Thus, the normalized correlated motion coefficient alone seems to be insufficient to represent the behavior of atoms. We then evaluated the distribution of the squared displacement and the result is shown in Figure 15. We see a few domains with the lower values of the squared displacement in this case, and these domains roughly correspond to the region of atoms with the highest values of the normalized correlated motion coefficient. The image obtained from the combination of those two figures roughly represents that obtained from observing the animation. It is worth noting that the trajectory in Figure 1b shows solid-like structure although the atomic arrangement in Figures 14 and 15, which is a snap shot, is more disturbed.

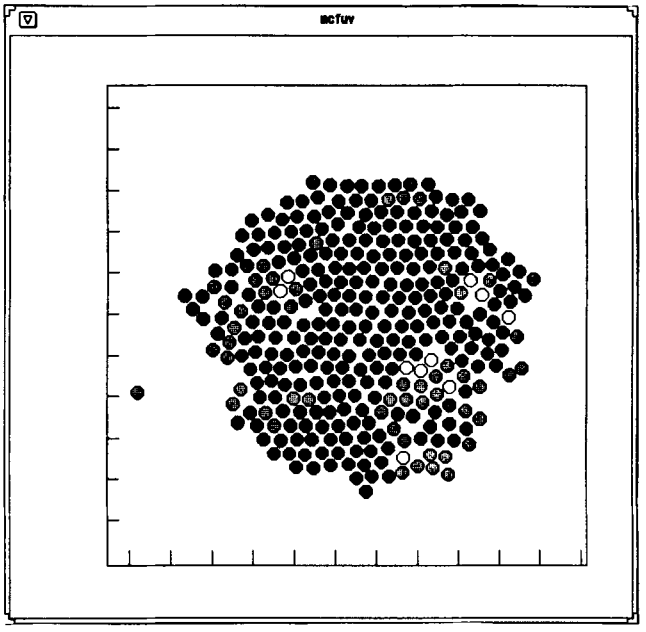

Figure 14 The gray scaled picture of the normalized correlated motion coefficient for the cluster at $T = 0.375\varepsilon/k_B$. The darker the gray level is, the larger the value of the coefficient. The white indicates negative values.

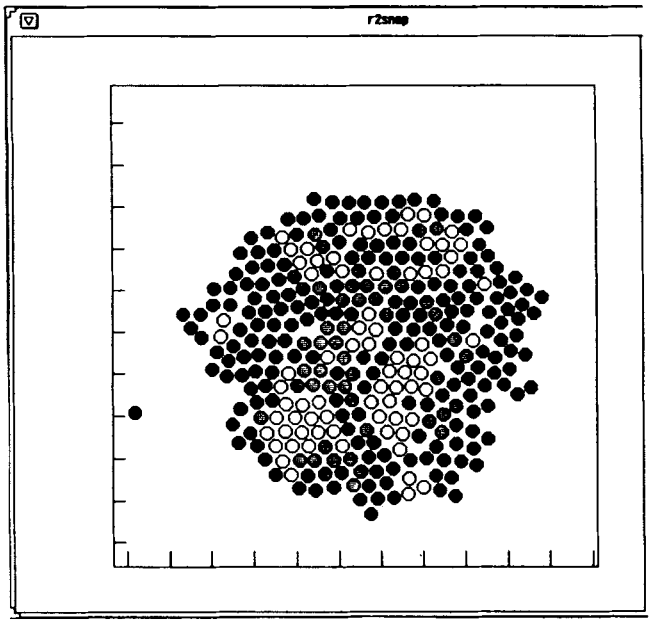

Figure 15 The gray scaled picture of the distribution of squared displacement for the same cluster as in Figure 14.

At $T = 0.417\varepsilon/k_B$, similar but much more vigorous behavior is observed as compared with that at $T = 0.375\varepsilon/k_B$. Thus, the mechanism of self diffusion in solid-like clusters involves collective motion of small domains and diffusion of atoms in the low density region created at the boundary of the domains. This is quite different from those in the bulk solid or in the bulk liquid. The value of the activation energy for clusters shown in Figure 7, which is twenty to thirty times larger than that for the bulk liquid, is consistent with this observation. This mechanism is also consistent with the jerky curve in Figure 3b and the solid-like spectra having non-zero densities at zero frequency as shown by the solid curves in Figures 12 and 13. At $T = 0.333\varepsilon/k_B$ these corrective motions are not observed.

4 CONCLUSION

Molecular dynamics simulation study is carried out to get insight into the mechanism of self diffusion which is characteristic of solid-like microclusters. A two-dimensional system is employed to facilitate visul analysis. The Lennard-Jones potential is assumed and the temperatures near the triple point of the two-dimensional bulk system are adopted for the simulation. The results show that:

a) microclusters consist of two regions, i.e., solid-like core and liquid-like surface regions,
b) the size dependence of the diffusion coefficient for microclusters is weak, and the value of the solid-like core region is not much different from that of the bulk liquid,
c) the activation energy of diffusion for microclusters is twenty to thirty times larger than that for the bulk liquid,

d) the diffusion mechanism in the solid-like region involves collective motion of small domains containing ten to twenty atoms which results in the formation of low density regions, sometimes even vacancy clusters, between them, and atoms in the low density regions change their positions to cause diffusion.

Acknowledgements

The authors wish to thank Mr. A. Mori, Mr. J. Tajima and Mr. R. Manabe of University of Tokushima for helping them in performing the simulation. This work is supported by a Grant in Aid for Scientific Research on Priority Areas "Crystal Growth Mechanism in Atomic Scale" under Grant No. 0343101 and No. 04227108, which is provided by the Ministry of Education, Science and Culture in Japan.

References

[1] C. Kaito, Y. Saito and K. Fujita, "Ordered structure in alloy grains of iron-nickel produced by the gas evaporation technique", *Jpn. J. Appl. Phys.*, **28**, L694 (1989).
[2] C. Kaito and Y. Saito, "Ordered Grains produced by Coalescence of *Fe* and *Ni* Smoke Grains", *Proc. Japan Acad.*, **65**, Ser. B, 125 (1989).
[3] C. Kaito, "Coalescence Growth of Smoke Particles Prepared by a Gas-Evaporation Technique", *Jpn. J. Appl. Phys.*, **17**, 601 (1978).
[4] C. Kaito, "Formation of Double Oxides by Coalescence of Smoke Particles of Different Oxides", *J. Cryst. Growth.* **55**, 273 (1981).
[5] C. Kaito, "Electron Microscope Study of Alloy Particles Produced by the Coalescence of Al Smoke and Cu Smoke", *Jpn. J. Appl. Phys.*, **23**, 525 (1984).
[6] C. Kaito, "Coalescence Growth Mechanism of Smoke Particles", *Jpn. J. Appl. Phys.*, **24**, 261 (1985).
[7] K. Kimoto, Y. Kamiya, M. Nonoyama and R, Uyeda, "An electron microscope study of fine metal particles prepared by evaporation in argon gas at low pressure", *Jpn. J. Appl. Phys.*, **2**, 702 (1963).
[8] C. Kaito and Y. Saito, "Iron-Nickel Ordered Grains Produced by the Reaction of Metallic Film and Ultrafine Metallic Grains", *J. Geomag. Geoelectr.*, **42**, 1241 (1990).
[9] L. Neel, L. Pauleve, R. Pautlenet, J. Laugier and B.D. Dautreppe, "Magnetic properties of an iron-nickel single crystal ordered by neutron bombardment", *J. Appl. Phys.*, **35**, 873 (1964).
[10] A. Chamberod, J. Laugier and J.M. Penisson, "Electron irradiation effects on iron-nickel invar alloys", *J. Magn. Mater.*, **10**, 139 (1979).
[11] J. Jellinek, T.L. Beck and S. Berry, "Solid-liquid phase changes in simulated isoenergetic Ar13", *J. Chem. Phys.*, **84**, 2783 (1986).
[12] P.M. Ajayan and L.D. Marks, "Quasimelting and Phases of Small Particles", *Phys. Rev. Lett.*, **60**, 585 (1988).
[13] H. Mori, M. Komatsu, K. Takeda and H. Fujita, "Spontaneous alloying of copper into gold atom clusters", *Phil. Mag, Lett.*, **63**, 173 (1991).
[14] H. Yasuda, H. Mori, M. Komatsu, K. Takeda and H. Fujita, "In situ observation of spontaneous alloying in atom clusters", *J. Electron Microsc.*, **41**, 267 (1992).
[15] H. Yasuda, H. Mori, M. Komatsu and K. Takeda, "Alloying behavior of gold atoms into nm-sized copper clusters", *Appl. Phys. Lett.*, **18**, 2173 (1992).
[16] H. Yasuda, H. Mori, M. Kamatsu and K. Takeda, "Spontaneous alloying of copper atoms into gold clusters at reduced temperatures", *J. Appl. Phys.*, **73**, 1100 (1993).
[17] H. Yasuda and H. Mori, "Spontaneous alloying of zinc atoms into gold clusters and formation of compound clusters", *Phys. Rev. Lett.*, **69**, 3747 (1992).
[18] H. Mori and H. Yasuda, "Formation of $AuSb_2$ compound clusters by spontaneous alloying", *Intermetallics*, **1**, 35 (1993).
[19] F.F. Abraham, "Melting in two dimensions is first order: an isothermal-isobaric Monte Carlo study", in *Ordering in Two Dimensions*, ed. S.K. Sinha, (Elsevier North Holland, Inc., New York, 1980), pp 155–161.
[20] T. Muranaka and Y. Hiwatari, private communication.
[21] A. Ueda, "Computer Simulation" [in Japanese], (Asakurasyoten, Tokyo, 1990).